Determination of Interfacial Area in Gas-Liquid Two Phase by Light Transmission

Ghiassi, Seied Hossein; Safekordi, Ali Akbar*⁺; Babazadeh Shareh, Fatemeh

Faculty of Chemical & Petroleum Engineering, Sharif University of Technology, Tehran, I.R. IRAN

ABSTRACT: *The purpose of the present paper is to develop light beam method to measurement of interfacial area in a rectangular gas-liquid bubble column. Total interfacial area can be determined in bubble column filled by transparent liquid by light transmission method. According to pervious researches, the fraction of parallel light is function of interfacial area and optical path length that these two parameters imply Transmission Number or N_T. The drop diameters were measured in the range of 2.2 to 5 mm, and in this range, the specific area is found to depend only upon the light transmission. Three different systems with various liquid phases have been used in this work. It had been proved that light transmission method for dilute suspension or stationary gas phase has a good consequence. In this work, good agreement between actual and calculated interfacial area proves that light transmission method would be able to determine interfacial area in multiple scattering, and it is possible to use earlier mathematic model to measure interfacial area in multiple scattering in gas-liquid bubble columns.*

KEY WORDS: *Light transmission, Interfacial area, Gas-liquid, Bubble column*

INTRODUCTION

Bubble column reactors are used extensively to perform a wide variety of gas-liquid or gas-liquid-solid reactions such as oxidation, hydrogenation, chlorination, aerobic fermentation, waste water treatment, and coal liquefaction [1-5]. The knowledge of bubble properties, including bubble velocity, bubble size, gas holdup, and specific interfacial area, are considerable importance for the proper design and operation of bubble columns. For example, the overall mass transfer rate per unit volume of dispersion in bubble column is governed by the liquid-side volumetric mass transfer coefficient ($K_l a$), assuming that the gas-side resistant is negligible. In a bubble column reactor, the variation in $K_l a$ is primarily due to variation in the specific interfacial area a.

The specific gas-liquid interfacial area, a, is related to the bubble size distribution and gas holdup, ε_g, while the gas holdup is determined by the bubble size distribution and bubble velocity. In the same way, bubble properties play key role in determining heat transfer rate in bubble column [6], but in most gas-liquid contacting equipments, interfacial area available for mass and heat transfer is usually indeterminate. In this way, direct measurement of Interfacial area can contribute to a better understanding of heat and mass transfer and their industrial applications. The light transmission is a well-developed direct technique for determining particle size and bubble size distribution [7-9]. In addition, bubble size itself is an important consideration, particularly in emulsion and

81

bubble phase, and it has often been adopted for measurement of interfacial area in liquid-liquid and gas-liquid dispersion [10-12]. The same data from interfacial area measurements will also give average drop size in terms of Sauter mean diameter. Several methods have been used to measure the interfacial area or drop size dispersion, but none of them seem to combine simplicity and accuracy. Various physical and chemical methods have been applied to measurement the specific interfacial area in multiphase flows. Physical methods include Gas Disengagement [13], Video Imaging [14-15], Laser Doppler Anemometry (LDA) [16], and special probes [17-18]. Chemical methods [16, 19, 20] are based on the study of reactions of known kinetics. Between all of them, light transmission method has been proven to be the simplest method.

THEORITICAL SECTION

When a parallel beam of light is passed through a transparent suspension or dispersion, light is scattered by particles of the dispersed phase by reflection, refraction, diffraction and absorption. If one drop is considered, the angular scattering of parallel rays can be pictured as in Fig. 1. The angular distribution and intensity of the scattered and transmitted light for dilute suspensions (no multiple scattering) has been calculated by *Mie* [21], and is thoroughly discussed by *Sinslair* [22]. Multiple scattering occurs when light which has been scattered by one drop is scattered again by another drop. For more concentrated dispersion, the above laws no longer hold because the light detector receives an excess amount of light. *Chu* [23] has shown the difficulties arising in trying to solve this case. Summarily, the error introduced by multiple scattering will be minimized if the light detector has a high angular resolution [8, 24]. Thus, with proper construction of the light detector, the effect of multiple scattering will not be significant, and the scattering cross section of the drops will be equal to the geometric cross section. More satisfactory techniques have been indicated by *Rose* [7]. In this, the optical system is so arranged that light scattered by reflection or refraction is not received by the photocell. This will be satisfied with arranging the photocell at large distance from the region of scattering light beam. As a result, scattered light passes outside the photocell and is small part of the incident parallel beam which has detected by the photocell. In this manner,
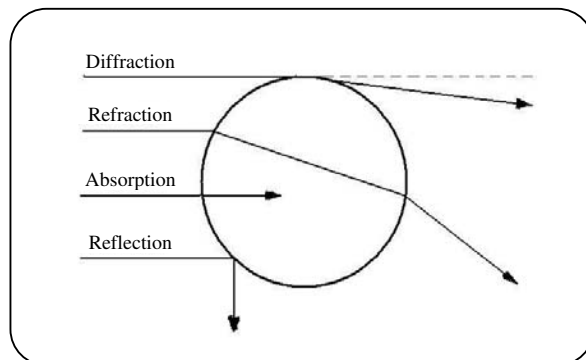

Fig. 1: Four mechanisms of light transmission.

the dispersed phase, as viewed by the photocell, appears as black discs and the amount of light received does not depend on the refractive indices of two phases or the condition of dispersed phase even if it is opaque or transparent.

To consider the dispersion geometry, Fig. 2 shows a parallel light beam incident on a circular volume of dispersion with dimensions R, L. If all of the drops are assumed to be spherical, which is a valid assumption for small drops, the volume fraction of dispersed phase is given by:

$$\varepsilon = \frac{\sum_{i=1}^{n} d_i^3}{6R^2 L} \tag{1}$$

The interfacial area per unit volume of dispersion for spherical bubbles of uniform size is:

$$a = \frac{6\varepsilon}{d_{32}} \tag{2}$$

Where d_{32} is the Sauter mean diameter of the drops:

$$d_{32} = \frac{\sum_{i=1}^{n} d_i^3}{\sum_{i=1}^{n} d_i^2} \tag{3}$$

To simulate the amount of light transmitted through this dispersion, the geometry may be reduced from 3D to 2D, and the Fig. 2 will be reduced to the Fig. 3.

Calderbank [10] presented an analysis of light transmission when unscattered light is received by photocell:

$$-dA = A.dl.a \tag{4}$$

$$\frac{-dA}{A} = dl.a \tag{5}$$

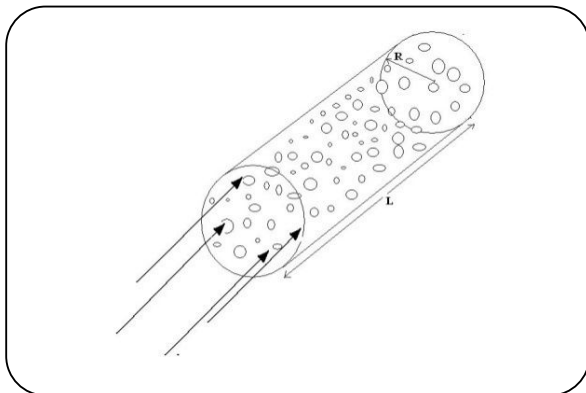82

Fig. 2: Light transmission path through a dispersion phase.

Fig. 3: -dimensional view.

$$-d \log_e A = a.dl \tag{6}$$

$$\log_e \frac{A_0}{A} = a.l \tag{7}$$

They considered that the shadow cast by each particle is infinitely long, and those particles in this shadow do not contribute to the scattering again.

$$\frac{I_0}{I} = \frac{A_0}{A} \tag{8}$$

Thus,

$$\log_e \frac{I_0}{I} = a \ .l \tag{9}$$

Or,

$$\log_{10} \frac{I_0}{I} = \frac{a.l}{9.21} \tag{10}$$

McLaughlin & Rushton [25] showed another analysis of light transmission through a dense dispersion of spherical particles when scattered nonparallel light was removed from the beam before it reached the photocell. They numerically generated samples from various drop size distribution and used a relation for the probability of a light ray nit struck every drops. They found that the total light transmission is a unique exponential function of a group al, where a is the interfacial per unit of volume, and l is the path length through the dispersion. The dimensionless group, defined here as the Transmission Number N_T, is:
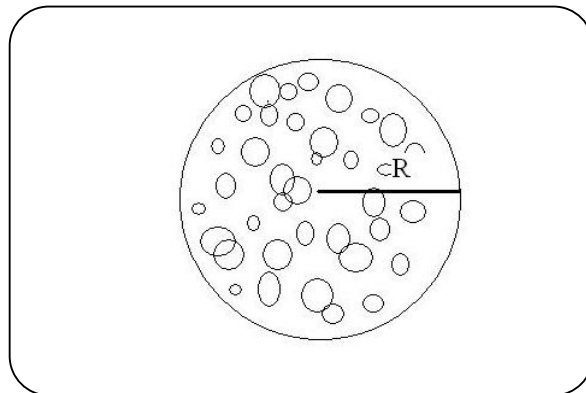
$$N_T = \frac{\varepsilon l}{d_{32}} \tag{11}$$

And *a* is defined:

$$a = \frac{6\varepsilon}{d_{32}} \tag{12}$$

With the combination of these two equations:

$$N_T = \frac{al}{6} \tag{13}$$

They denied that the probability of light transmission on a path, and therefore in a beam is a unique function of N_T regardless of the range of drop sizes. They obtained:

$$f = \exp(-1.5N_T) \tag{14}$$

We can simplify this equation and rewrite:

$$\log f = \log(\exp(-\frac{al}{4})) \tag{15}$$

$$\log \frac{1}{f} = \frac{1}{4} al \log e \tag{16}$$

$$\log \frac{1}{f} = \frac{al}{9.21} \tag{17}$$

f is the ratio of received light to incident light intensity, or the probability of light not being scattering from the path, thus it would be concluded:

$$f = \frac{I}{I_0} \tag{18}$$

After rearrangement:

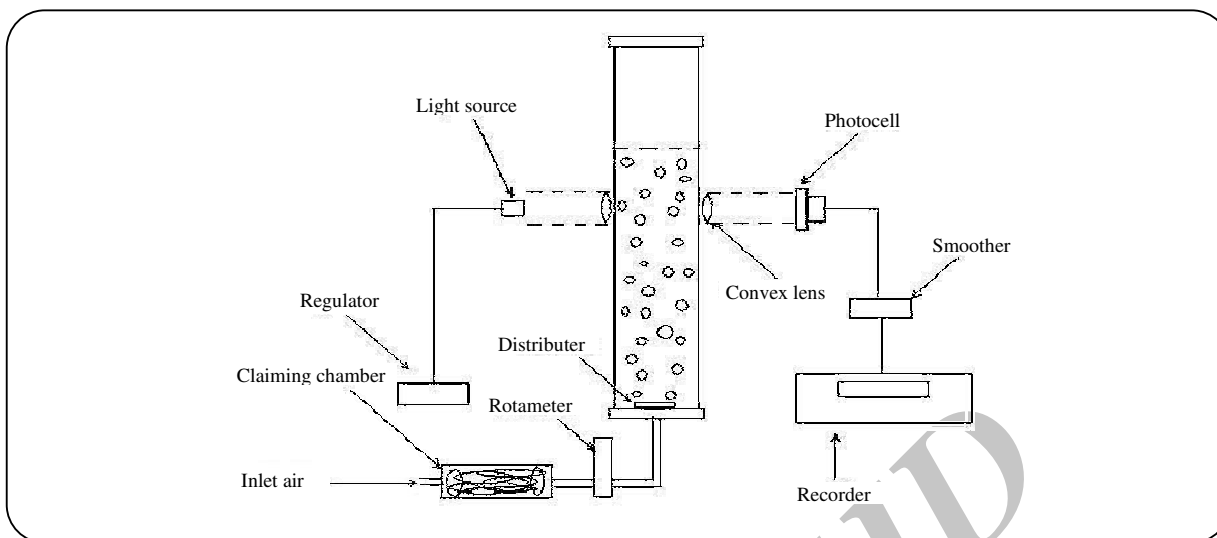$$\log_{10} \frac{I_0}{I} = \frac{a.l}{9.21} \tag{19}$$

83

Fig. 4: Schematic of the experimental set-up of bubble column.

Or,

$$a = \frac{9.21}{l}\log_{10}\frac{I_0}{I} \tag{20}$$

EXPERIMENTAL SECTION

Experiments were carried out in a rectangular glass bubble column of 10cm×10cm internal dimensions and approximately 100cm in long with a porous plate type gas distributor. The schematic of the experimental set-up is shown in Fig. 4. Air passes through acalm chamber containing with a porous media, allowing the air to be uniform. With this particular injection system, a uniform and monodisperse population of bubbles can be formed [26]. The column was separately filled with three solutions (distillated water only, distillated water and 30%wt glycerol, distillated water and 58%wt glycerol) as liquid phase which was stationary part. The gas phase (air) was introduced at the bottom of the column using porous plate gas distributor. The gas holdup was determined on the basis of froth height and clear liquid head level. The volumetric flow rate of air was measured with calibrated rotameter. The light source was a type of Hyperlight Lamp or LED. A set of lenses for producing a parallel beam of light and an A.C. voltage regulator was used to conduct the power to the lamp and control the intensity of the light produced. Voltage regulator was in series with a constant voltage and consequent changes in light intensity during a set of runs. Two lenses, double convex kind,

in series as shown in Fig 4, were set up to make parallel beam. The duty of one lens was making parallel beam and other one was receiving parallel beam. The diameter of each lens was 5 cm with the 10 cm focal length.

These two lenses were fixed at the height of 40cm of tower where the bubbles distribution is completely uniform. Each of two lenses in two sides of the column join the column wall thus the surrounding light does not enter into the lenses. The distance between lens and light source and also the other lens and photocell was covered with the opaque covering until light scattered by reflection and refraction was not received by the photocell. Scattered nonparallel light was thus removed from the beam before it reached the photocell. The specification of photocell is according to below:

Opening slit: 0-8 mm adjustable
Dimensions: 53 mm × 70 mm
Stand rod length: 13 Cm × 8 mm

The signal from the photocell was smoothed and was fed to the electronic measuring device. Furthermore, the output with volt format from the volt meter was recorded. In order to measure the required data, initiate voltage was recorded. Then, the volt format of volt meter output, which was received its signal from photocell, was recorded with this procedure. So, I_0 and I could be inscribed. The bubble diameter was measured by the photographic method. The air was entered into the column in different flow rates. In each flow rate,

the image of the column is taken in order to measure the diameters of bubbles correctly with the image analyzing.

RESULTS AND DISCUSSION

With the help of image analyzing, bubble size distribution is calculated. Fig. 5 typically shows the histogram of bubble size distribution for aqueous 30%wt glycerol for 1.8 (L/s) air flow rate. The results for bubble diameter measuring are depicted in Fig. 6. it shows the diagram of Sauter mean diameter relative to flow rate for three systems.

With increasing the gas phase flow rate, Sauter mean diameter of drops will raise. In addition, changing in continued phase nature, will lead to change in Sauter mean diameter of drops. Because of this, we will have limitation to reach the same holdup; so maximum holdup of each system is unique. The main reason of this phenomenon is that the surface tension will be varied.

With the use of Sauter mean diameter which was calculated, interfacial area can be calculated. After calculating the interfacial area, Eq. (19) can be used in order to compute the K coefficient. The result in Fig. 7 shows that the Eq. (19) is valid for three systems that we described them. The K coefficient is *Mie* [21] scattering factor which represents the ratio of light scattering cross-section of particles to actual cross-section of particles.

$$K = \text{Mie scattering factor} =$$

$$\frac{\text{light scattering cross-section of particles}}{\text{actual cross-section of particles}}$$

Fig. 7 indicates the $\log(I_0/I)$ versus al. According to Eq. (19), the slope of this depiction will result in K coefficient. As it is mentioned, K coefficient is the *Mie* factor which shows that how light scattering cross-section of particles is close to actual cross-section of particles. For three systems, K is calculated. For distilled water-air we have, K=0.94 for al<14.4. As al varies from 0 to 14.4, gas holdup varies from 0 to 12%. For aqueous 30%wt glycerol, the result indicates that K=1.04 for al<12.8 and gas holdup varies from 0 to 5.8%. For aqueous 58%wt glycerol, the result indicates that K=0.99 for al<8.1 and gas holdup varies from 0 to 3.5%. The results are depicted in Fig. 8, where the interfacial area calculated from the light reading (Eq.20) is plotted against the actual interfacial area of the bubble column
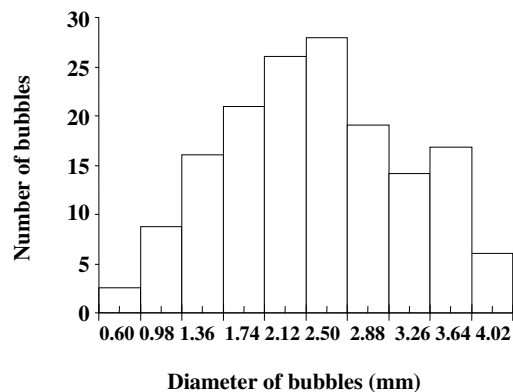

Fig. 5: Bubbles size distribution for 1.8(lit/s) Air into distillated water- 30%wt glycerol.
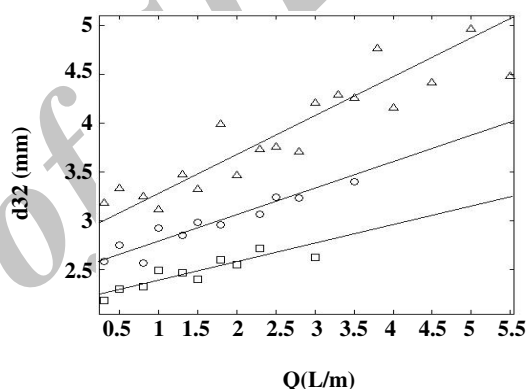

Fig. 6: Sauter mean diameter relative to flow rate △ Distillated water-Air, □ Aqueous 30%wt glycerol-Air, ○ Aqueous 58%wt glycerol-Air.
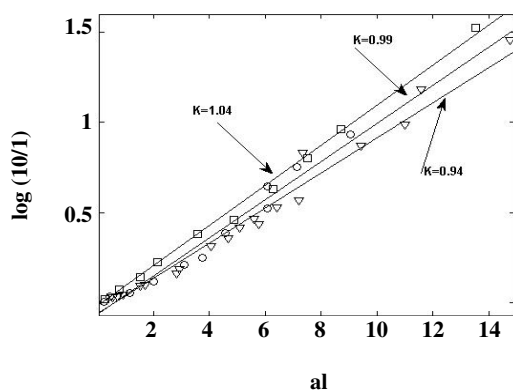

Fig. 7: Experimental results for light received by the detector as a function of interfacial area, △ Distillated water-Air, □ Aqueous 30%wt glycerol-Air, ○ Aqueous 58%wt glycerol-Air.
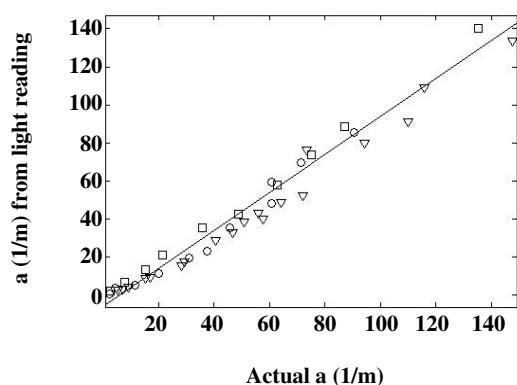
85

Fig. 8: Calculated versus actual interfacial area, △ Distillated water-Air, □ Aqueous 30%wt glycerol-Air, ○ Aqueous 58 wt glycerol-Air.

(Eq.(12)). It is so obvious that the actual interfacial area and the calculated interfacial area have a good agreement with each other. Fig. 8 adequately shows that (Eq. (20)) describes the light transmission characteristics of all bubbles dispersions regardless of size distribution or volume fraction is used. Thus the result of mathematical model was verified to experiment results.

CONCLUSIONS

Fig. 8 proves that light transmission method can be used to calculate the interfacial area in gas-liquid bubble column. Not with standing the fact that the light transmission has been demonstrated to use in dilute suspension, it is possible to use this method to calculate the interfacial area in multiple scattering when light which has been scattered by one drop is scattered again by another drop.

Acknowledgments

Nomencluture

A_0	Cross section area of light beam, m^2
A	Free area at any cross section in light beam, m^2
a	Interfacial area, $1/m$
d_i	Diameter of any bubbles, mm
d_{32}	Sauter mean diameter of drops, otherwise called the area average diameter, mm
f	The fraction of light transmitted through a dispersion
I_0	Incident light intensity, v
I	Transmitted light intensity, v
l	Optical path length, m
N_T	Transmission number, dimensionless
R	The radius of light beam cross section, m

Greek Letter

ε	Volume fraction of gas phase

REFERENCES

[1] De Swart j.W.A., Krishna R., Effect of Article Concentration on the Hydrodynamics of Bubble Column Slurry Reactors, *Chem. Eng. Res. Design., Trans. Ind. chem. Eng.*, **73**, p. 308 (1995).

[2] Jager B., Espinoza R., Advances in Low Temperature Ficher-Tropsch Synthesis, *Catalyst Today*, **23**(1), p. 17 (1995).

[3] Shollenberger K.A., Torczynski J.R., Adkins D.R., O'Hem T., Jakson N.B., Gamma-Densitometery Tomography of Gas Holdup Spatial Distribution in Industrial Scale Bubble Column, *Chem Eng Sci.*, **52**, p. 2037 (1997).

[4] Eishenberg B., Ansel L.L., Fiato R.A., Bauman R.F., Advanced Gas Conversion Technology for Remote Natural Gas Utilization, *GPA Convention, New Orleans*, LA (1994).

[5] Davis B.H., Overview of Reactor for Liquid Phase Fischer-Topsch Synthesis, *Catalyst Today*, **71**(3-4), p. 249 (2002).

[6] Yang G.Q., Luo X., Lao R., Heat-Transfer Characteristics in Slurry Bubble Columns at Elevated Pressures and Tempratures, *Ind. Eng. Chem. Res.*, **39**, p. 2568 (2000).

[7] Rose H.E, H.B. Lloyd, On The Measurement of the Size Characteristics of Powders by Photo-Extenction Methods 1. Theoretical Consideration, *J. Soc. Chem. Ind.*, **65**, p. 5 (1946).

[8] Boll R.H., C.M. Sliepcevich., Evaluation of Error of Optical Origin Arising in the Size Analysis of Dispersion by Light Transmission, *J. Opt. Soc. Am.*, **46**, p. 200 (1956).

[9] Dobbins R.L., Jizmagian G.S., Optical Scattering Cross Sections for Polydispersions of Dielectric Sphere, *AIChE J.*, **20**, p. 184 (1974).

[10] Calderbank P.H., Physical Rate Process in Industrial Fermentation, Part 1 : The Interfacial Area in Gas-Liquid Contacting with Mechanical Agitation, *Trans. Inst. Chem. Engrs*., **36**, p. 443 (1958).

[11] Lee J.C., Ssali, G.W.K., Bubble Transport and Coalescence in a Vertical Pipe , Joint Meeting on Bubble and Foams, S1-6.1 , Verfahrenstechnische Gesellschaft im VDI Inst., *Chem. Engrs., Nurenberd* (1971).

[12] Trice V.G., Rodger W.A., Light Transmittance as a Measure of Interfacial Area in Liquid-Liquid Dispersion, *AIChE J.*, **2**, p. 205 (1956).

[13] Patel S.A., Daly J.G., Bukur D.B., Bubble Size Distribution in Fischer-Tropsch Waxes in a Bubble Column, *AIChE J.*, **36**, p. 93 (1996).

[14] Akita K., Yoshida F., Gas Holdup and Volumetric Mass Transfer Coefficient in Bubble Columns. Effect of Liquid Properties, *Ind. Eng. Chem. Process. Des. Dev.*, **12**, p.76 (1974).

[15] Luewisutthichat, Tsutsumi, Zdrojkowski, Bubble Cractristics in Multi-Phase Flow Systems: Bubble Sizes and Size Distribution*, J. Chem. Eng. Jpn.*, **30**, p. 461 (1999).

[16] Kulkarni A.A., Joshi J.B., Kumar V.R., Kulkarni B.D., Simultaneous Measurement of Holdup Profiles and Interfacial Area Using LDA in Bubble Column : Predictions by Multiresolution Analysis and Comparison with Experiments, *Chem. Eng. Sci*., **56**, p. 6437 (2001).

[17] Kiambi S.L., Duquenne A.M., Bascoul A., Delmas H., Measurements of Local Interfacial Area: Application of Bi-Optical Fiber Technique, *Chem Eng Sci*., **56**, p. 6447 (2001).

[18] Wu Q., Ishii M., Sensitivy Study on Double-Sensor Conductivity Probe for the Measurement of Interfacial Area Concentration in Bubbly Flow, *Int. J. Multi Flow*, **25**, p. 155 (1994).

[19] Stegman D., Knop P.A., Wijnads A.J.G., Westertern K.R. Interfacial Area and Gas Holdup in a Bubble Column Reactor at Elevated Pressure, *Ind. Eng. Chem. Res*., **35**, p. 3842 (1996).

[20] Vazquez G., Cancela M.A., Riverol C., Alvarez E., Navaza J.M., Determination of Interfacial Areas in a Bubble Column by Different Chemical Methods, *Ind. Eng. Chem. Res.,* **39**, p. 2541 (2000).

[21] Mie P., *Ann.Pys. Lpz.*, **33**, p. 1275 (1910).

[22] Sinclair D., "Handbook of Aerosols", Ch. 7, Washington , D.C. :Atomic Energy Commission (1950).

[23] Chiao-Min-Chu., *J. phys. Chem*., **59**, p. 841 (1955).

[24] Sheppard P.A., The Effect of Pollution on Radiation in the Atmosphere, *Intern. J. Air pollut*., **1**, p. 31 (1958)

[25] McLaughlin C.M., Rushton J.H., Interfacial Area of Liquid-Liquid Dispersion from Light Transmission Measurements, *AIChE J*., **19**, p.817 (1973).

[26] Garnier C., Lance M., Marié,J., Measurement of Local Flow Characteristics in Buoyancy-Driven Bubbly Flow at High Void Fraction, *Experimental Thermal and Fluid Science*, **26**, p. 811 (2002).